

to decouple Eq. (1). The adjoint of Eq. (4) is

$$\{Z'\} = -[A]^T \{Z\} \quad (9)$$

with the following associated boundary conditions:

$$\{Z\}^T \{Y\} \Big|_{-a/2}^{a/2} = 0 \quad (10)$$

A formal solution of Eq. (9) is given by

$$\{Z\} = [C] \begin{bmatrix} e^{-\lambda_1 x_1} & & 0 \\ & \ddots & \\ 0 & & e^{-\lambda_n x_1} \end{bmatrix} \{n\} \quad (11)$$

where $[C]$ denotes the matrix of eigenvectors of $-[A]^T$.

Substitution of Eq. (11) into the corresponding boundary conditions of the adjoint problem at the edges $x_1 = \pm a/2$ results in a homogeneous algebraic equation of the form

$$[E]\{n\} = 0 \quad (12)$$

We have to solve for the eigenvector $\{n\}$ corresponding to each frequency ω .

Making use of the following biorthogonality conditions of the natural modes with respect to the eigenfunctions $\{Y_m\}$ and $\{Z_n\}$,

$$-\int_{-a/2}^{a/2} \{Z_n\}^T [M] \{Y_m\} dx_1 = M_m \delta_{mn} \quad (13)$$

$$\int_{-a/2}^{a/2} \{Z_n\}^T (\{Y'_m\} - [K]\{Y_m\}) dx_1 = \omega_m^2 M_m \delta_{mn} \quad (14)$$

and substituting Eq. (2) into Eq. (1), performing left multiplication by the adjoint eigenfunction $\{Z_n\}^T$, and integrating over the domain, we obtain

$$\ddot{T}_m(t) + \omega_m^2 T_m(t) = \frac{1}{M_m} \int_{-a/2}^{a/2} \{Z_m\}^T \{r_m\} dx_1 \quad (15)$$

For zero initial conditions, the state vector $\{y\}$ will be expressed as

$$\begin{aligned} \{y_m(x_1, t)\} &= \frac{1}{M_m} \{Y_m(x_1)\} \int_0^t h_m(t - \tau) \\ &\times \int_{-a/2}^{a/2} \{Z_m\}^T \{r_m(\xi, \tau)\} d\xi d\tau \end{aligned} \quad (16)$$

where $h_m(t - \tau)$ is the impulse response function.

Numerical Results and Discussion

The numerical applications are carried out for cross-ply spherical shells whose geometrical and material properties are the same for all layers. The transverse deflection presented in the figures is evaluated at $(x_1, x_2, \xi) = (0, b/2, \xi)$. Zero initial conditions are assumed. The variations of center deflection with time for antisymmetric cross-ply (0/90) and symmetric cross-ply (0/90/0) laminated spherical caps are shown in Figs. 1 and 2, respectively, for various boundary conditions. It is interesting to note that for SSSS, SSCS, and SCCC boundary conditions the amplitudes are smaller for symmetric cross-ply than for antisymmetric cross-ply laminates, whereas for SSFF, SSFS, and SSFC the amplitudes are higher. Moreover, the first-order (FSDT) and the third-order (HSDT) theories predict almost the same response,

whereas the classical theory (CST) differs both in amplitude and phase.

Reference

- Reddy, J. N., and Liu, C. F., "A Higher Order Shear Deformation Theory of Laminated Elastic Shells," *International Journal of Engineering Science*, Vol. 23, 1985, pp. 319-330.

Vibration of Clamped Right Triangular Thin Plates: Accurate Simplified Solutions

H. T. Saliba*

Lakehead University,
Thunder Bay, Ontario P7B 5E1, Canada

Nomenclature

- a = plate dimension in x direction
- b = plate dimension in y direction
- D = flexural rigidity of plate, $Ek^3/12(1 - \nu^2)$
- E = Young's modulus of plate material
- h = plate thickness
- k = number of terms used in solution
- k^* = upper limit for first summations of solutions
- W = plate lateral displacement divided by side length a
- η = distance along plate y axis divided by side length b , y/b
- λ^2 = eigenvalue, $\omega a^2 \sqrt{\rho/D}$
- ν = Poisson's ratio of plate material
- ξ = distance along plate x axis divided by side length a , x/a
- ρ = mass of plate per unit area
- ϕ = plate aspect ratio, b/a
- ω = circular frequency of plate vibration

I. Introduction

USE of the superposition techniques in the free-vibration analyses of thin plates, as they were first introduced by Gorman,¹ has provided simple and effective solutions to a vast number of rectangular plate problems. The method has also been extended to nonrectangular plates such as triangular and trapezoidal plates. However, serious difficulties were encountered in some of these analyses. These difficulties were discussed and obviated in Ref. 2. This reference, however, dealt only with simple support conditions, leading to a simple, highly accurate, and very economical solution to the free-vibration problem of simply supported right angle triangular plates.

The purpose of this Note is to show that the modified superposition method of Ref. 2 is also applicable to clamped-edge conditions. This is accomplished through the application of this method to the title problem.

II. Mathematical Procedure

The solution is similar in every aspect to that of the simply supported right angle triangular plate of Ref. 2. It is based on the principles of superposition. In this method, a number of appropriate building blocks, for which Lévy-type solutions are readily available or easily obtainable, are superimposed. The contributions of these building blocks to the various boundary conditions of the original plate are formulated. Finally, the coefficients appearing in these formulations are adjusted to satisfy the prescribed edge conditions of the plate under study. Depending on its aspect ratio, the right angle

Received Oct. 12, 1993; revision received July 6, 1994; accepted for publication July 6, 1994. Copyright © 1994 by the American Institute of Aeronautics and Astronautics, Inc. All rights reserved.

*Professor, Department of Mechanical Engineering. Senior Member AIAA.

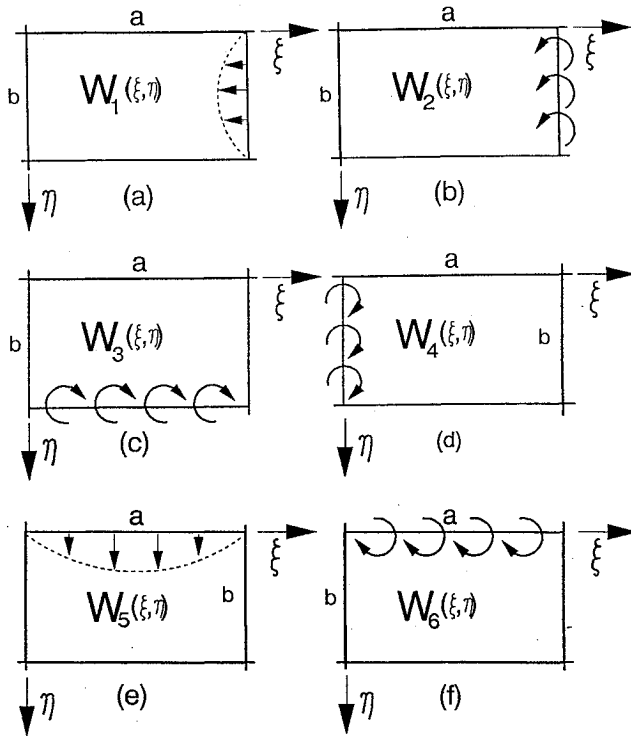


Fig. 1 Building blocks used in the solution of fully clamped right triangular plates.

triangular plate with clamped-edge conditions is analyzed by superimposing either four or all six of the building blocks of Fig. 1. This is discussed in more detail in the following sections.

III. Building Blocks

The building blocks used here are the Lévy-type solutions of plates a-f of Fig. 1. Extended edges in this figure indicate simple support conditions. Straight arrows, or straight arrows with a dashed arc, indicate zero moment and a forced harmonic edge displacement. Curved arrows, on the other hand, indicate zero displacement and a forced harmonic moment. The first plate of Fig. 1, or plate a, has three of its edges simply supported. The fourth edge, $\xi = 1$, has zero moment and a forced edge displacement given by

$$\lim_{k \rightarrow \infty} W_1(1, \eta) = \sum_{m=1,2,\dots} E_{1m} \sin(m\pi\eta)$$

In view of these boundary conditions, the Lévy-type solution for this plate is

$$W_1(\xi, \eta) = \sum_{m=1,2,\dots}^{k^*} E_{1m} \theta_{11m} [\sinh(\beta_m \xi) + \theta_{1m} \sin(\gamma_m \xi)] \sin(m\pi\eta) + \sum_{m=k^*+1}^{\infty} E_{1m} \theta_{22m} [\sinh(\beta_m \xi) + \theta_{2m} \sinh(\gamma_m \xi)] \sin(m\pi\eta)$$

where the first summation pertains to values of $\phi^2 \lambda^2 > (m\pi)^2$, and where $\beta_m = (1/\phi) \sqrt{\phi^2 \lambda^2 + (m\pi)^2}$ and $\gamma_m = (1/\phi) \sqrt{\phi^2 \lambda^2 - (m\pi)^2}$ or $(1/\phi) \sqrt{(m\pi)^2 - \phi^2 \lambda^2}$, whichever is real, and where

$$\theta_{1m} = \frac{[\beta_m^2 - \nu(1/\phi)^2(m\pi)^2] \sinh \beta_m}{[\gamma_m^2 + \nu(1/\phi)^2(m\pi)^2] \sin \gamma_m},$$

Table 1 Comparison of the first six mode eigenvalues, $\lambda^2 = \omega a^2 \sqrt{\rho/D}$, with existing published data

| Mode | Source | b/a | | |
|------|---------|--------|--------|--------|
| | | 1 | 2 | 3 |
| 1 | Present | 93.790 | 53.444 | 42.756 |
| | Ref. 3 | 93.86 | 53.45 | 42.76 |
| | Ref. 4 | 93.789 | 53.447 | 42.756 |
| 2 | Present | 157.79 | 82.425 | 60.993 |
| | Ref. 3 | 157.7 | 82.42 | 60.99 |
| | Ref. 4 | 157.79 | 82.431 | 61.000 |
| 3 | Present | 194.76 | 113.51 | 80.660 |
| | Ref. 3 | 194.8 | 113.5 | 80.66 |
| | Ref. 4 | 194.77 | 113.51 | 80.809 |
| 4 | Present | 242.80 | 121.85 | 99.696 |
| | Ref. 3 | 242.8 | 121.9 | 99.68 |
| | Ref. 4 | 242.80 | 121.92 | 99.908 |
| 5 | Present | 277.68 | 151.56 | 103.13 |
| | Ref. 3 | — | — | — |
| | Ref. 4 | 277.67 | 152.09 | 104.12 |
| 6 | Present | 335.65 | 167.98 | 132.47 |
| | Ref. 3 | — | — | — |
| | Ref. 4 | 335.77 | 168.68 | 129.69 |

Table 2 First four mode eigenvalues, $\lambda = \omega a^2 \sqrt{\rho/D}$, for fully clamped right triangular plates with aspect ratios, b/a, as shown

| b/a | Mode | | | |
|------|--------|--------|--------|--------|
| | 1 | 2 | 3 | 4 |
| 1.25 | 76.089 | 126.47 | 159.34 | 191.98 |
| 1.50 | 65.460 | 106.21 | 139.08 | 158.00 |
| 1.75 | 58.431 | 92.381 | 125.25 | 135.64 |
| 2.25 | 49.747 | 75.008 | 102.72 | 113.49 |
| 2.50 | 46.885 | 69.263 | 93.768 | 107.97 |
| 2.75 | 44.610 | 64.701 | 86.549 | 103.57 |

$$\theta_{2m} = - \frac{[\beta_m^2 - \nu(1/\phi)^2(m\pi)^2] \sinh \beta_m}{[\gamma_m^2 - \nu(1/\phi)^2(m\pi)^2] \sinh \gamma_m}$$

$$\theta_{11m} = \frac{1}{(\sinh \beta_m + \theta_{1m} \sin \gamma_m)},$$

$$\theta_{22m} = \frac{1}{(\sinh \beta_m + \theta_{2m} \sinh \gamma_m)}$$

The second plate, or plate b, has three simply supported edges. Its fourth edge, $\xi = 1$, has zero displacement and a forced edge harmonic moment given by

$$\lim_{k \rightarrow \infty} \frac{M_n a^2}{bD} = \sum_{m=1,2,\dots}^k E_{2m} \sin(m\pi\eta)$$

Its Lévy-type solution is

$$W_1(\xi, \eta) = \sum_{m=1,2,\dots}^{k^*} E_{2m} \theta_{11m} (\sinh \beta_m \xi + \theta_{1m} \sin \gamma_m \xi) \sin(m\pi\eta) + \sum_{m=k^*+1}^{\infty} E_{2m} \theta_{22m} (\sinh \beta_m \xi + \theta_{2m} \sinh \gamma_m \xi) \sin(m\pi\eta)$$

where β_m and γ_m are as defined earlier and where

$$\theta_{1m} = - \frac{\sinh \beta_m}{\sin \gamma_m}, \quad \theta_{11m} = - \frac{1}{(\beta_m^2 \sinh \beta_m - \theta_{1m} \gamma_m^2 \sin \gamma_m)}$$

$$\theta_{2m} = - \frac{\sinh \beta_m}{\sinh \gamma_m}, \quad \theta_{22m} = - \frac{1}{(\beta_m^2 \sinh \beta_m + \theta_{2m} \gamma_m^2 \sinh \gamma_m)}$$

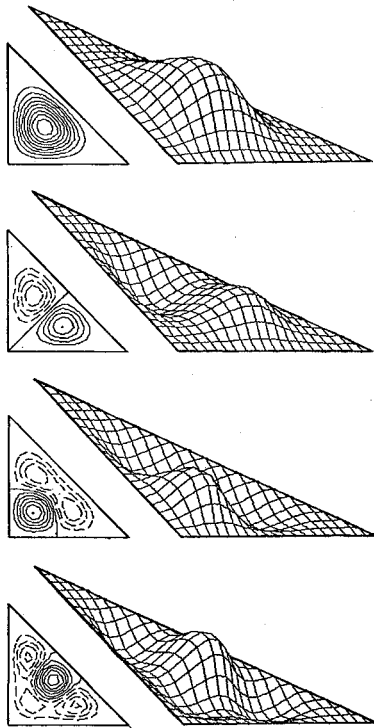


Fig. 2 First four contour plots and mode shapes for a plate with aspect ratio $b/a = 1.0$.

Symbols are as defined in the Nomenclature. It is easily seen here that the solutions for plates c, d, and f are obtained from that of plate b through simple transformation of the axes. Similarly, the solution of plate e is inferred from that of plate a.

IV. Superposition of the Building Blocks

Now that the solutions of plates a–f of Fig. 1 are in place, their contributions to the clamped boundary conditions of the right triangular plate of interest are formulated. The procedure is similar to that of Ref. 2. The results are computer coded and stored in subroutines that are called as required. Consequently, these formulations need never be repeated. The reader is reminded here that conditions along the hypotenuse, diagonal of the full rectangular plate, are controlled by the forcing functions prescribed along edge 2, $\xi = 1$, or edge 3, $\eta = 0$, of the rectangular plate. Consequently, it was stressed in Ref. 2 that, to achieve the required convergence, the prescribed harmonic lateral displacement and the prescribed harmonic moment must act along the longest of these two edges. This proved to be adequate when dealing with simple support conditions. Although necessary, this condition proved not to be sufficient in the case of clamped-edge conditions, when the plate aspect ratio is close to unity. It quickly became apparent that, in this case, the contribution of the prescribed functions along edge 2, $\xi = 1$, and along edge 3, $\eta = 0$, to conditions along the diagonal (hypotenuse) are of the same order of magnitude. Consequently, two additional building blocks are used in the solution of these plates, i.e., plates with aspect ratios between 0.5 and 2.0.

A. Plates with Aspect Ratios Between 0.5 and 2.0

For these plates, all six building blocks of Fig. 1 are used in the solution. These building blocks are superimposed on top of each other. It is seen here that the zero displacement conditions along the two edges, $\xi = 0$ and $\eta = 1$, are readily satisfied. Satisfying the remaining four conditions, i.e., zero slope along all three edges and zero displacement along the third edge (hypotenuse), leads to a set of $6k$ linear algebraic equations. Written in matrix form, and requiring the determinant of the coefficient matrix to vanish, these equations lead to the frequency equation.

B. Plates with Aspect Ratios Less Than 0.5 or Greater Than 2.0

For these plates, only four building blocks are required for the solution. For plates with aspect ratios $b/a \geq 2.0$, the first four building blocks of Fig. 1 are used. For plates with aspect ratios $b/a \leq 0.5$, the last four building blocks of Fig. 1 are used. Satisfaction of the boundary conditions here leads to a set of $4k$ homogeneous algebraic equations resulting in a coefficient matrix of $4k \times 4k$ as oppose to $6k \times 6k$ in the previous case. An attempt to use six building blocks here leads to numerical instabilities.

V. Numerical Results and Concluding Remarks

Numerical analyses confirmed that six building blocks are necessary for the analysis of clamped plates with aspect ratios ϕ such that $0.5 < \phi < 2.0$. However, only four building blocks must be used for clamped plates with aspect ratios ϕ such that $\phi \leq 0.5$ or $\phi \geq 2.0$. Furthermore, to generalize this technique, the solution of simply supported plates of Ref. 2 was re-examined. It was reconfirmed that, in this case, only two building blocks were necessary for the generation of eigenvalues, regardless of the aspect ratio of the plate. However, although not necessary, it was found that the use of four building blocks, in the solution of simply supported right triangular plates with aspect ratios between 0.5 and 2.0, led to smoother shapes. It is for this reason that the author recommends the use of building blocks a, b, e, and f of Fig. 1 in the solution of simply supported right triangular plates with aspect ratios between 0.5 and 2.0 exclusively. For plates with aspect ratios $b/a \geq 2$, building blocks a and b are to be used. For plates with aspect ratios $b/a \leq 0.5$, building blocks e and f have to be used. Numerical analyses proved that this practice leads to greater numerical stability.

In Table 1, numerical results obtained using the modified superposition techniques discussed in this paper are compared with those of Gorman³ as well as those of Kim and Dickinson.⁴ Although all three sets of results are in general agreement, the superiority of the present technique is in its simplicity and its adaptability to the solution of other, more complicated shapes and boundary conditions. The method, although analytical in nature, lends itself very well to simple computational techniques for the generation of eigenvalues and mode shape data.

In brief, the solution technique presented in this paper represents a noticeable improvement over existing methods. It is a significant advance in the superposition method. It leads to a highly accurate simplified solution to the title problem. It has all of the advantages of the superposition solution presented by Gorman.³ At the same time, it eliminates all of the disadvantages of Gorman's solution as were discussed by him in this reference. False eigenvalues referred to by Gorman as "rejection modes" are virtually eliminated by the present method of solution.

The first four eigenvalues for a wide range of plate aspect ratios are given in Table 2. Because of space limitation, mode shapes are limited to a plate of aspect ratio 1 as shown in Fig. 2. This solution has been computer coded and is available from the author on request.

Acknowledgment

The author wishes to acknowledge the financial support of the Natural Science and Engineering Research Council of Canada.

References

- Gorman, D. J., *Free Vibration Analysis of Rectangular plates*, Elsevier, North-Holland, New York, 1982.
- Saliba, H. T., "Transverse Free Vibration of Simply Supported Right Triangular Thin Plates: A Highly Accurate Simplified Solution," *Journal of Sound and Vibration*, Vol. 139, No. 2, 1990, pp. 289–297.
- Gorman, D. J., "Free Vibration Analysis of Right Triangular Plates with Combinations of Clamped-Simply Supported Boundary Conditions," *Journal of Sound and Vibration*, Vol. 106, No. 3, 1986, pp. 419–431.
- Kim, C. S., and Dickinson, S. M., "The Free Flexural Vibration of Right Triangular Isotropic and Orthotropic Plates," *Journal of Sound and Vibration*, Vol. 141, 1990, pp. 291–311.